Journal of Food Composition and Analysis 149 (2026) 108688

Contents lists available at ScienceDirect

Journal of Food Composition and Analysis

journal homepage: www.elsevier.com/locate/jfca

AIEgen-based metal-organic framework probe enhancing fluorescence and antibody activity in lateral flow immunoassay for zearalenone detection

Chengchen Pang [a,b,c], Keyun Ren [a,b,c], Haitao Xu [a,b,c], Kunying Nie [a,b,c], Chunlei Yu [a,b,c], Daohong Zhang [d], Qingqing Yang [a,b,c,*]

[a] School of Agricultural Engineering and Food Science, Shandong University of Technology, No. 266 Xincun West Road, Zibo 255049, People's Republic of China
[b] Shandong Provincial Engineering Research Center of Vegetable Safety and Quality Traceability, No. 266 Xincun West Road, Zibo 255049, People's Republic of China
[c] Zibo City Key Laboratory of Agricultural Product Safety Traceability, No. 266 Xincun West Road, Zibo 255049, People's Republic of China
[d] College of Food Engineering, Ludong University, Yantai, Shandong 264025, People's Republic of China

ARTICLE INFO

Keywords:
Lateral flow immunosensor
Point-of-care detection
MOF@AIEgens
Zearalenone

ABSTRACT

To enable on-site detection of ZEN toxin in agricultural samples, an POC LFIA detection method based on monoclonal antibody was established through an advanced MAF materials. AIEgens have garnered significant attention for their unique fluorescence properties at high concentrations, overcoming the ACQ limitation of traditional luminescent materials. MAF is a Zr^{4+}-based AIE metal-organic framework that amplifies AIEgen fluorescence and enables crosslinker-free antibody assembly through its intrinsic affinity for antibodies. This preserves antibody activity while ensuring detection sensitivity through targeted Fab exposure. The MAF-LFIA exhibited good linearity with an ultralow limit of detection of 0.0021 ng/mL (approximately 0.42 ng/g in corn samples), a cut-off value of 5 ng/mL, and recoveries of 99.9–102.3 % in cornmeal. These results indicated that this platform provides a robust strategy for real-time monitoring of food contaminants in complex matrices.

1. Introduction

Zearalenone (ZEN) is a mycotoxin that is commonly found in agricultural products and is known for its potent estrogenic toxicity (Obremski et al., 2016; Wang et al., 2018b). It is produced by the F. graminearum and Gibberella fungi, posing serious health risks to both humans and livestock (Zhang et al., 2020a). Moreover, ZEN exhibits remarkable stability during food storage and processing due to its resistance to environmental changes and heat treatment, making its removal challenging (Zielonka et al., 2020). Therefore, there is an urgent need to develop a novel point-of-care (POC) detection method.

The POC Lateral flow immunoassay (LFIA) technology enables rapid detection of small molecules by exploiting the change in signal intensity caused by the specific binding of antibodies to target analytes. Owing to their portability, rapid response, and suitability for decentralized testing, POC biosensors have been increasingly applied in on-site healthcare diagnostics, food and water safety monitoring, and rapid antimicrobial or drug detection (Gopal et al., 2021). Fluorescent switches, characterized by high sensitivity, fast response, and good selectivity, have recently attracted great attention in the field of sensors (Pršir et al., 2023). Several LFIAs for zearalenone detection have been reported, and some commercial test strips are already available. Most fluorescent test strips in current research employ quantum dots and lanthanide materials as alternative fluorescent probes due to their superior optical properties (Zhu et al., 2023). Yet under high-concentration or solid-state conditions, these materials still exhibit fluorescence loss issues-wherein planar fluorescent molecules readily undergo intense π-π stacking interactions, thereby triggering the aggregation-caused quenching ACQ phenomenon (Zhang et al., 2023).

Aggregation-induced emission luminogens (AIEgens) have emerged as a new class of fluorescent probes with strong emission in the aggregated or solid state. More recently, AIEgens have attracted extensive interest due to their luminous fluorescent properties in bulk or in high concentrations, which could overcome the disadvantages (ACQ) of conventional luminescent materials (Chua et al., 2023; Snigdhamayee et al., 2024). Due to the fact that AIEgens have strong fluorescent properties due to their rotating and non-radiation suppression, the more concentrated AIEgens are, the more luminous they become (Mei et al.,

* Corresponding author at: School of Agricultural Engineering and Food Science, Shandong University of Technology, No. 266 Xincun West Road, Zibo 255049, People's Republic of China.
E-mail address: yqqing@sdut.edu.cn (Q. Yang).

https://doi.org/10.1016/j.jfca.2025.108688
Received 21 August 2025; Received in revised form 22 November 2025; Accepted 27 November 2025
Available online 28 November 2025

2015; Zhang et al., 2020b).

Several AIEgen-based LFIAs have been reported, demonstrating remarkable sensitivity due to the unique aggregation-induced emission and photostability of AIEgens (Zhang et al., 2024). Recently, Janus plasmonic-AIE hybrid nanobeads (J-cf-HBN) were constructed by integrating gold nanoparticles with AIEgens and, after conjugation with monoclonal antibodies, were employed in immunochromatographic assays for the ultrasensitive detection of staphylococcal enterotoxin B (SEB) in milk (Shen et al., 2024). However, direct conjugation of ultra-fine AIEgen nanocrystals to antibodies can induce partial denaturation or steric hindrance of antigen-binding sites, impairing antibody bioactivity and reducing assay reproducibility. In addition, ultra-fine AIEgen nanocrystals often face challenges in achieving stable conjugation and efficient release from the lateral flow membrane, limiting their practical application in LFIA (Bian et al., 2022). To overcome these limitations, this study designed a metal-AIEgen framework (MAF) by coordinating Zr^{4+} with AIEgens, forming a stable fluorescent platform capable of self-assembling with antibodies while maintaining their functional conformation and enhancing signal stability.

Metal-Organic Frameworks (MOFs) are characterized by their stable framework, excellent structural, and high-temperature and chemical stability (Pang et al., 2023). Since the Fab region (fragment of antigen-binding) of the antibody plays a key role in recognizing the target substance, it is crucial to ensure its targeted exposure during probe preparation. The Zr^{4+}-based organometallic framework can self-assemble with antibodies through simple mixing. During this process, the Fc region of the antibody is embedded within the pores of the MOF, while the Fab region remains exposed outside the framework (Alt et al., 2022; Wang et al., 2023). Several studies have demonstrated that MOF-antibody (MOF-Ab) assemblies protect antibody activity and facilitate targeted exposure of the Fab region, thereby ensuring high assay sensitivity (Caihong et al., 2018; Feng et al., 2019; Wang et al., 2018a; Zhang et al., 2020c). More recently, antibody-conjugated MOFs have been applied to optical immunosensing of environmental pollutants; for example, an NH_2-MIL-101(Fe)-based fluorescent probe functionalized with anti-Pb^{2+} monoclonal antibodies enabled rapid and highly selective detection of lead ions in water, with a limit of detection of 9.51 ppb and satisfactory recoveries in real samples (Singh et al., 2024).

The luminescence mechanism of AIEgen is particularly compatible with MOFs, as the metal ions in MOFs can restrict the rotation and vibration of AIEgen, thereby enhancing fluorescence signals (Zhang et al., 2022). In this study, a Metal-organic framework (MAF) material with fluorescent properties was prepared via a solvothermal method using Zr^{4+} as the metal center and a light-emitting polymer AIEgen as the organic ligand. Because MAF combines the properties of both MOFs and AIEgens, it can amplify the luminescence of AIEgens through the anchoring effect of Zr^{4+}, while also enabling simple self-assembly with antibodies, preserving their bioactivity and ensuring targeted exposure of the Fab region. The ZEN monoclonal antibody was directly mixed with MAF to form the MAF-Ab complex, which served as the recognition element for rapid and highly sensitive detection of zearalenone (ZEN) using a competitive lateral flow immunoassay (LFIA) format. Overall, this work aims to develop a portable, highly sensitive, and stable fluorescent LFIA system for on-site monitoring of ZEN contamination in agricultural products.

2. Materials and methods

2.1. Materials

ZEN monoclonal antibody was provided by Qingqing Yang's group. The classical AIEgen substances Tetracarboxylic acid tetraphenylethylene (TCPE) and $Zrcl_4$ were purchased from Macklin Biotechnology Co., Ltd. ZEN-BSA antigen and Goat anti-mouse IgG (H+L) were purchased from Biodragon Co., Ltd. OTA, DON, AFB1 and FB1 standards were purchased from Tianjin Alta Biological Co., Ltd. NC membrane, gold labeling pad and absorbent pad were purchased from Shandong Lvdu Biological Co., Ltd. DMF and acetic acid were analytically pure and purchased from Aladdin Bio Co., Ltd.

2.2. Preparation of MAF

The MAF material was prepared by the classical solvothermal method. Briefly, the classical 96 mg of AIEgen material (TCPE) and 23 mg of Zirconium Chloride ($Zrcl_4$) were dissolved in 6 mL of N,N-Dimethylformamide (DMF) solution, and 2 mL of acetic acid (CH_3COOH) was added as a structure-directing agent. The mixture was then heated in an oil bath at 90 °C for 4 h with continuous magnetic stirring to ensure thorough mixing. A white precipitate appeared in the solution in about 1 h, and the precipitated material was the prepared MAF material. When the white precipitate was no longer produced, it meant that the reaction was finished and sufficient MAF material had been produced in the solution. The suspension was centrifuged at 7200 ×g for 15 min, and the precipitate was washed twice with DMF and ethanol. The final product was resuspended in ethanol and stored at 4 ℃ or freeze-dried into powder.

2.3. Characterization and infrared determination of MAF morphology

MAF powder was dispersed in ethanol and diluted to an appropriate concentration. A portion of the dispersion was placed on a copper grid and air-dried for transmission electron microscopy (TEM) to examine its morphology. The samples were sprayed with gold and subjected to scanning electron microscopy (SEM) and energy spectrum scanning. A portion of the sample was dispersed into ethanol solution for ultrasonication, and then a few drops of the dispersed liquid were added drop by drop on the mica sheet, and after drying, the sample was photographed with an AFM instrument (The equipment is provided by Scientific Compass), with a scanning range of 1 μm*1 μm to observe the microscopic state of the surface as well as its roughness. The samples were prepared in the form of potassium bromide pressed tablets for infrared spectroscopy in the range of 400–4000 cm^{-1}.

2.4. Preparation of MAF-ZEN-Ab

Since MAF has properties similar to those of MOF organometallic framework analogs, it has a high affinity for antibodies. Therefore, the MAF material can be coupled with the antibody in the form of electrostatic adsorption to protect the activity of the antibody as much as possible. 20 mg of MAF was resuspended in PBS (pH = 7.4), sonicated for 1 min to fully disperse it, and then washed twice with PBS buffer solution under centrifuge conditions (7200 ×g, 10 min). 10 μL (1 mg/mL) of ZEN monoclonal antibody was added to the resuspended MAF, and then shaken well and placed in a shaker for 2 h (37 ℃) to make MAF and ZEN monoclonal antibody bind well. 100 μL of 20 mg/mL BSA solution was taken for blocking, and the reaction was continued in a shaker for 1 h. After blocking, the reaction was centrifuged at 16100 ×g for 15 min, and washed twice with PBS.

2.5. Test strip assembly

The POC sensor was prepared by dry test strip method (Pang et al., 2024). The assembly of the test strip was divided into three parts, laying the gold standard pad on the NC film and then finally laying the sample pad to complete the assembly of the test strip. Firstly, the treatment of the gold standard pad, to ensure the drying of the gold standard pad will be placed in the 37 ℃ oven to dry for half an hour first. 1 mL of successfully coupled time-resolved fluorescent probe was added dropwise onto a 30 cm gold-labeled septum and dried at 37 ℃ for 2 h. ZEN-BSA (1 mg/mL) and Goat anti-mouse IgG (0.5 mg/mL) were sprayed onto the NC membrane at a concentration of 0.7 μL/cm respectively to

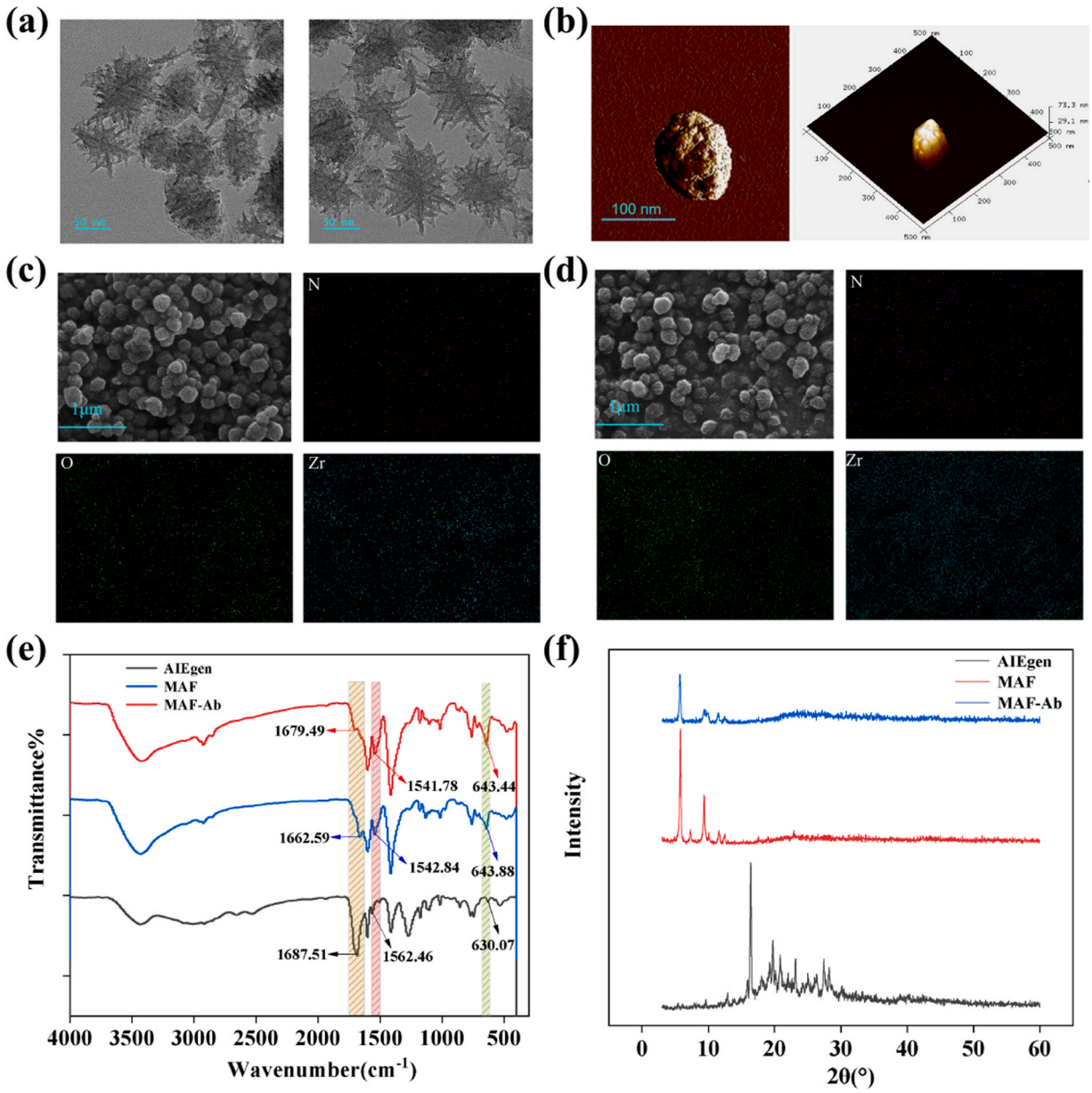

Fig. 1. Morphological and structural characterization of MAF and MAF-Ab. (a) Transmission electron microscopy (TEM) image of MAF. (b) Two-dimensional and three-dimensional atomic force microscopy (AFM) images of MAF. (c, d) Scanning electron microscopy (SEM) images and elemental analysis of MAF and MAF-Ab, respectively. (e) FT-IR spectra of MAF and MAF-Ab. (f) XRD patterns of MAF and MAF-Ab.

generate the test line and control line. The NC membrane was dried at 37 °C for 4 h. The absorbent pad, gold labeling pad, and sample pad were then attached to the substrate sequentially. Finally, the assembled strip was segmented into 3.8 mm TRFIAs using a microcomputer-controlled cutter and packaged in sealed bags with desiccants. When stored in desiccant-filled packaging, test strips can maintain their performance for weeks to months, demonstrating excellent stability.

2.6. Optimization of test strips

In order to achieve the best use of the prepared POC sensors, we optimized three factors that significantly affect the sensitivity of the test strips: the amount of monoclonal antibody, the amount of luminescent material MAF and the amount of MAF-Ab.

2.7. Performance of POC test strips

To verify the effect of POC test strips, 80 μL of PBS buffer solution was added to the microtiter wells at the end of test strip assembly. The color development effect was observed at an excitation wavelength of 365 nm after incubation in an oven for 5 min, and photos were taken using Iphone 13 pro. The fluorescence intensity of the T and C lines on the test strips was quantitatively analyzed by measuring the grayscale values (RGB) using ImageJ software. This approach enabled objective and reproducible evaluation of the colorimetric changes, allowing precise comparison of signal intensities under different experimental conditions.

2.8. Sensitivity

Standards of 5, 2.5, 1.25, 0.625 and 0.315 ng/mL were added to the test strips to determine the critical value and limit of detection (LOD) for

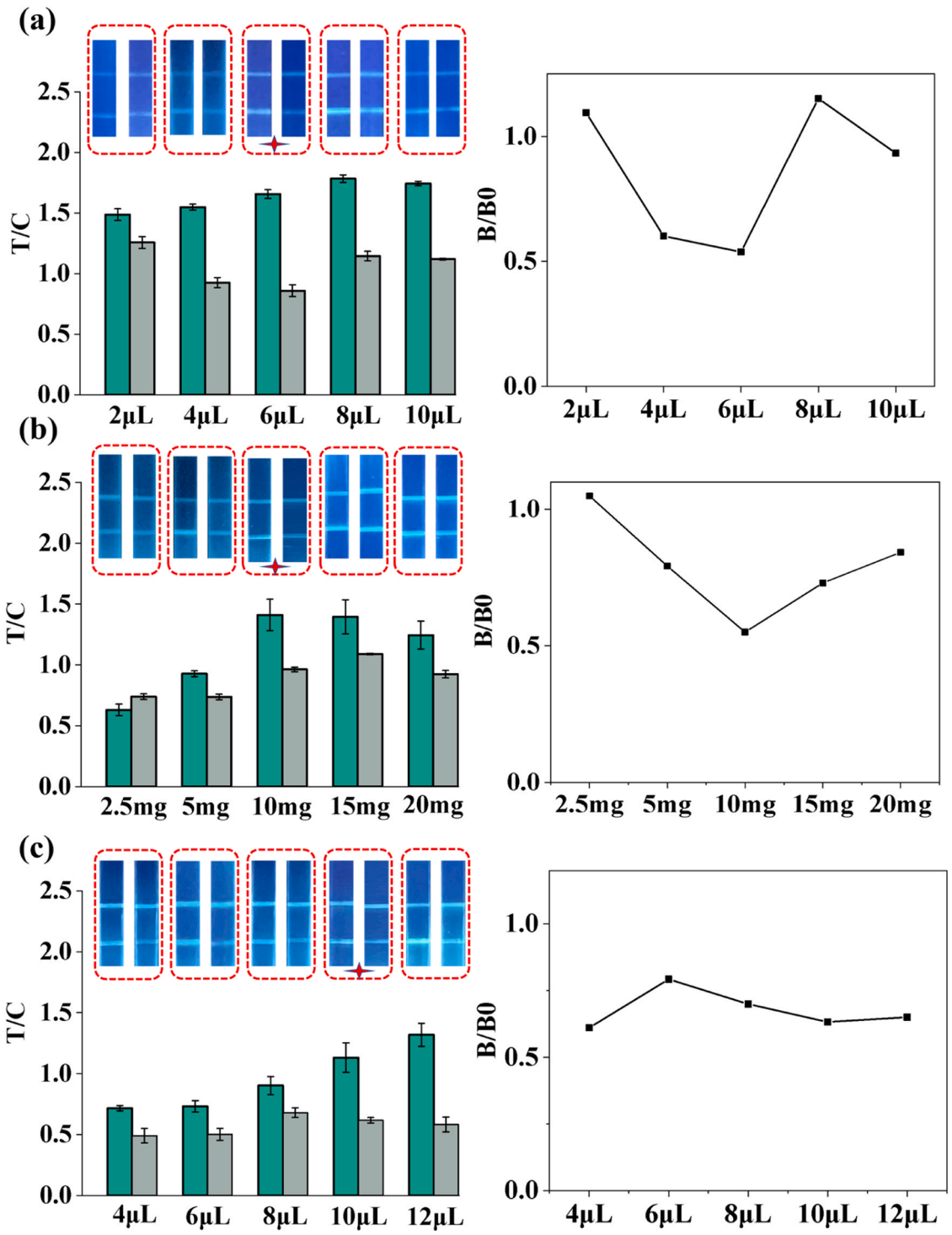

Fig. 2. Optimization of assay conditions for the POC test strips. (a) Optimization of Ab dosage. (b) optimization of MAF dosage. (c) optimization of MAF-Ab dosage. For each panel, the graphs on the left show the T/C values at different dosages, and the graphs on the right show the corresponding normalized responses (B/B0). (Error bars represent standard deviations, n = 3.).

the POC test strip assay. The point at which the T-line disappeared from visualization after addition of the standard was defined as the critical value.

The standard curve for the assay was derived using the logarithm of the concentration of the ZEN standard as the x-axis and B/B0 as the y-axis, with B in B/B0 representing the gray value of the T-line in the test strip and B0 representing the gray value of the C-line. The LOD value was calculated by Eq. (1). In the formula "δ" represents the SD of the ZEN test value between 20 negative samples, and "s" represents the slope of the calibration curve.

$$LOD = 3\delta / s \quad (1)$$

2.9. Specificity

To evaluate the specificity of the POC test strips, different target standards (AFB1, OTA, and DON) were spiked into cornstarch samples at a concentration of 2.5 ng/mL, and the color development was observed to assess the specificity of the method.The cross-reaction (CR) rate is calculated by Eq. (2)

$$CR(\%) = IC_{50}\ (ZEN) / IC_{50}\ (Othercarbamate\ pesticide) \times 100 \quad (2)$$

2.10. Actual sample accuracy and reproducibility

In order to test the accuracy and reproducibility of the POC sensor, we spiked cornmeal with known concentrations of ZEN standards and assayed them in triplicate, calculating their recoveries and coefficients of variation (CVs), and comparing them with the results of the instrumental method, the LC-MS/MS method.

2.11. Stability of POC test strip sensors

In order to ascertain the stability of the POC test strips under harsh environmental working conditions, the pH of the buffer, salt concentration, and methanol concentration were varied. The T1/T2 values of the test strips after the addition of 2 ng/mL of standard were used as a standard to verify their sensitivity.The degree of variability in methanol concentration ranged from 15 % to 95 %, while that of salt concentration spanned from 0.1 to 3.2 mol/L, and pH values fluctuated between 1 and 12.

2.12. Data analysis

All measurements were taken at least three times.Duncan's method was used to compare significant differences between the data. Data were statistically analyzed using SPSS 22.0 software. $P < 0.05$ indicates significant difference between data.

3. Results and analysis

3.1. The principle of the MOF@AIEgens-assisted POC LFIS

MOF materials are popular among interested parties due to their stable framework structure, which usually consists of a metallic ligand and an organic ligand, with the metallic ligand as the center and the organic ligand as the linker (Zhu and Xu, 2014; Hou et al., 2020).

In this study, a sea urchin-shaped MOF material with fluorescent properties (MAF) was prepared experimentally using Zr^{4+} as a metal ligand and AIEgen as an organic ligand through a solvothermal method. The anchored effect of Zr^{4+} on AIEgen enhances the aggregation-induced emission (AIE) effect, amplifying the fluorescence intensity of the MAF. MAF materials exhibit high affinity for antibodies (Yin et al., 2022), allowing facile construction of MAF-Ab through simple self-assembly. The MAF-Ab emits a bright blue color when excited at a wavelength of 365 nm, with intensity significantly enhanced in the aggregated state. The experiment utilized the competitive principle to establish a point-of-care test strip assay for detecting ZEN small molecule toxins. Goat anti-mouse antibody and ZEN-BSA were immobilized on the C and T lines of the test strip, respectively. When MAF-Ab aggregated on the T and C lines, a bright blue color was emitted. As the concentration of the standard in the solution increases, MAF-Ab will compete with the standard for binding, weakening the blue color on the T-line. The sample solution will flow from the T line to the C line due to the fiber effect of the test strip. Negative samples are indicated by a blue T line with no color change, while positive samples are indicated by an obvious weakening of the blue on the T line. The images were captured with an Apple iPhone 13 Pro and analyzed quantitatively using ImageJ software.

3.2. Characteristics of the MAF

As shown in Fig. 1a, the transmission electron microscopy (TEM) revealed that MAF has a sea urchin-like spherical shape with a diameter of approximately 100 nm and uniform size. Fig. 1b (AFM) imaging showed that the surface of MAF is rough and porous, providing the basis for self-assembly with the antibody and the targeted exposure of the Fab recognition region. As shown in Fig. 1c and d, scanning electron microscopy (SEM) imaging confirmed the rough and a uniform surface of MAF. Elemental analysis (EPS) indicated no change in the elemental composition of MAF after binding to the antibody.

3.3. FTIR analysis

Fig. 1e showed that AIEgen has an absorption peak at 1562.46 cm^{-1}, indicating the presence of an aromatic benzene ring C═C structure, consistent with the findings of Zhu Z et al. (Zhu et al., 2022). In the MAF sample, a shift in the peak position occurred at 1500–1600 cm^{-1}, indicating the occurrence of C═C stretching vibration of the benzene ring. Additionally, an enhancement in the absorption peak intensity at 643.88 cm^{-1} indicates a C-H bending vibration of the benzene ring. The stretching of the C═O functional group occurred at 1662.59 cm^{-1}, indicating the coordination reaction of Zr^{4+} with the COOH group of AIEgen. MAF showed a new peak at 1730 cm^{-1}, indicating the carboxylate COOH coordination bonding of Zr^{4+} with AIEgen. The FTIR spectra of sample MAF-Ab did not change significantly, suggesting that the attachment of the ZEN monoclonal antibody to the MAF does not alter the chemical bonding but merely inserts the antibody into the wells to achieve a mosaic assembly of antibody and MAF (Zhang et al., 2022).

3.4. The Optimization of MAF POC LFIA conditions

The MAF-Ab probe was formed by self-assembly of MAF with anti-ZEN monoclonal antibody. To optimize the performance of the probe and determine the optimal conditions for the POC LFIS method, the amounts of MAF, Ab, and MAF-Ab were adjusted. The T/C and B/B0 values of the blank test strips and those with added standards were used as criteria to evaluate strip performance (Pang et al., 2023).

MAF is the luminescent material on the POC LIFA test strips. The concentration of MAF conjugated to the antibody is a key determinant of fluorescence on the test strips. To achieve the optimal inhibition ratio while minimizing background interference, the MAF dosage to 2.5, 5, 10, 15, and 20 mg. The Fig. 2a indicated that the optimal inhibition effect was achieved at a dosage of 10 mg. However, when the dosage of MAF exceeds 15 mg resulted in noticeable background interference on the test strip.

The optimal concentration of antibody (Ab) was determined to achieve sufficient brightness on the T-line while maintaining an effective inhibition effect on the test strip. The Fig. 2b showed that the color of the T and C lines is too faint when the Ab concentration was 2 μL, whereas the inhibition effect reached its maximum at an antibody concentration of 6 μL. Further increasing the monoclonal antibody concentration to 8 μL did not result in a significant change in T-line brightness upon the addition of the ZEN standard, indicating that excessively high antibody concentrations can saturate the signal and limit the inhibition effect.

After determining the optimal dosage of MAF and Ab, the amount of MAF-Ab probes was further optimized. Fig. 2c showed that the inhibition effect was maximized when 10 μL of MAF-Ab was used. Higher probe dosages led to significant background interference, which negatively affected assay performance.

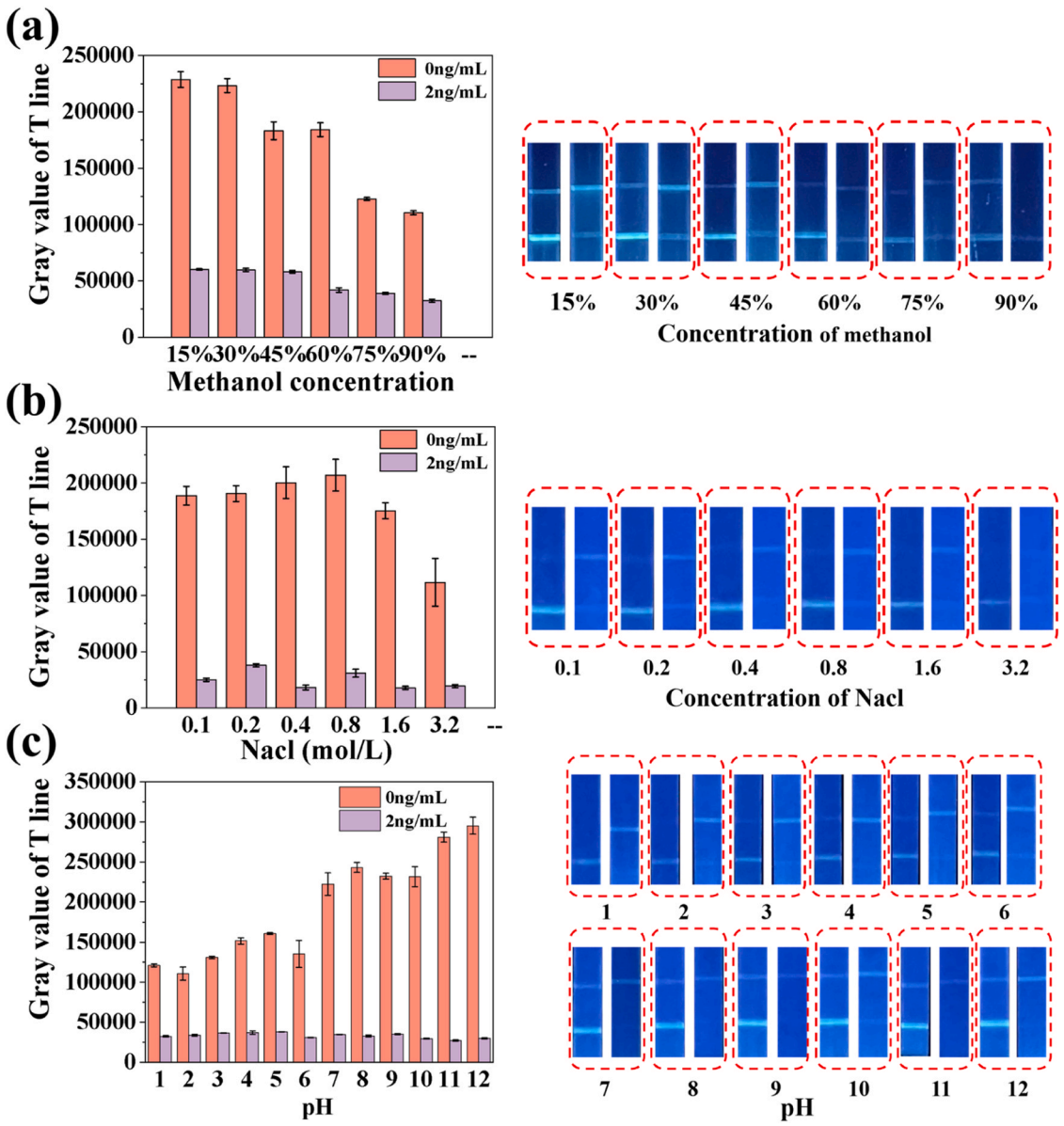

Fig. 3. Stability of the POC test strips under different assay conditions. (a) Methanol concentration. (b) Salt concentration. (c) pH. For each panel, the graphs on the left show the grayscale intensity of the T line under each condition, and the images on the right show the corresponding test strips, where the left and right test lines represent 0 and 2 ng/mL ZEN, respectively. (Error bars represent standard deviations, n = 3.).

3.5. Environmental tolerance of MAF POC LFIA methods

Antibodies are inherently sensitive and can lose activity under adverse conditions, which may significantly compromise the sensitivity of test strips (Pang et al., 2023). During applications with food samples, exposure to high concentrations of acids, bases, salts, or organic solvents can adversely affect monoclonal antibody activity. Therefore, it is crucial to evaluate the protective effect of MAF on antibodies. In this study, the tolerance of the test strip to harsh environments was assessed by monitoring the color change upon introduction of a 2 ng/mL standard (Wu et al., 2024).

As illustrated in the accompanying Fig. 3, when the test strip is subjected to a challenging environment, the brightness of the C and T lines of the test strip simultaneously diminishes. It is also noteworthy that the brightness of the C line is more susceptible to change, while the brightness of the T line remains relatively stable. Consequently, the gray value of the T-line prior to and subsequent to the addition of the standard was employed as a metric to assess its stability. This may be attributed to the protective effect of the MAF material on the ZEN antibody, while the secondary antibody of the C line lost its activity due to direct exposure to the harsh environment.

As illustrated in Fig. 3a, the color of the lower C-line exhibited a pronounced shift towards lighter hues when the methanol concentration reached 75 %. As illustrated in Fig. 3b, the POC strips are capable of withstanding a salt concentration of up to 0.8 mol/mL. As illustrated in Fig. 3c, the brightness of the T-line gradually increases with increasing pH, indicating that the POC strips can tolerate highly alkaline environments. In contrast, the MAF material loses its protective effect on the monoclonal antibody in highly acidic environments.

3.6. The performance of POC LFIA

The sensitivity and specific performance effects of the test strips are crucial parameters for evaluating their performance in detecting positive samples. Standard ZEN solutions at concentrations of 5, 2.5, 1.25, 0.625, and 0.315 ng/mL were applied to the sample pads of the test

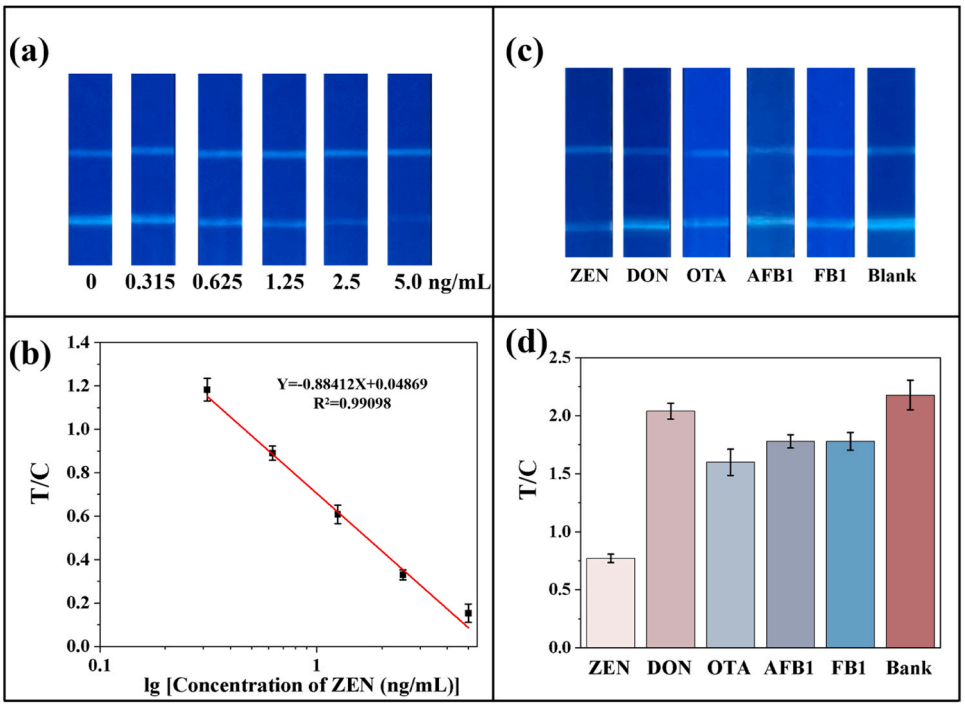

Fig. 4. Sensitivity and specificity of the MAF-LFIA test strips. (a) Fluorescence images of test strips for ZEN standards at different concentrations. (b) Corresponding T/C ratios as a function of ZEN concentration for the strips shown in (a). (c) Fluorescence images of test strips exposed to different mycotoxins (ZEN, DON, OTA, AFB1, FB1 and blank) at a standard ZEN concentration of 2.5 ng/mL. (d) Quantified T/C ratios for the strips shown in (c). Error bars represent standard deviations (n = 3).

Table 1
Recovery of ZEN in maize samples using the developed MAF POC test strip method.

Sample	Spiked level (ug/kg)	Detected concentration (Averaged ±SD)	Recover (%)	CV (%)
Cornflour	5.0	4.97 ± 0.09	99.92	1.8
	10.0	9.99 ± 1.02	99.97	10.2
	60.0	61.41 ± 2.52	102.3	4.09

strips under optimal working conditions. The strips were then incubated in the oven for 5 min and irradiated with a searchlight at an excitation wavelength of 365 nm. Fig. 4a and b showed that the fluorescence brightness of the T-line gradually decreased with increasing standard concentration, indicating that the ZEN monoclonal antibody on the T-line preferentially bound to free ZEN rather than to the immobilized ZEN-BSA conjugate. A calibration curve was constructed by plotting the standard concentrations on the x-axis and the T/C fluorescence intensity ratios on the y-axis, yielding a good linear relationship ($R^2 = 0.9907$) with the equation $Y = -0.88412 + 0.04869X$. The limit of detection (LOD) of the developed assay was determined to be 0.0021 ng/mL, and the cut-off value was 5 ng/mL.

To evaluate the specificity of the developed test strips, standards (OTA, DON, AFB1, FB1) at concentrations of 2.5 ng/mL were added to the test strips shown in Fig. 4c and d.

As illustrated in Fig. 4c, both the T line and C line displayed bright blue colouration regardless of whether the four interfering mycotoxins are added. However, upon addition of ZEN, the fluorescence intensity of the T line significantly decreased, while the C line remained clearly visible. Quantitative analysis in Fig. 4d revealed that the T/C ratio was markedly lower following ZEN addition compared with that of the other four mycotoxins. These results indicate negligible cross-reactivity between ZEN and the non-target mycotoxins, confirming the excellent selectivity and specificity of the MAF-assisted POC LFIS toward ZEN detection.

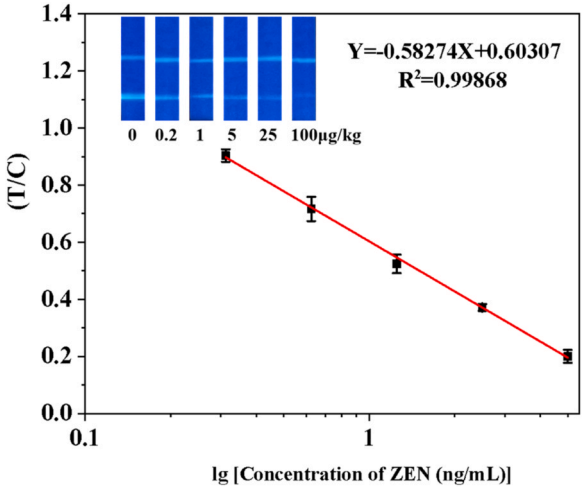

Fig. 5. Responses of the MAF assisted POC LFIS to different concentrations of ZEN spiked in Cornmeal.

The accuracy and stability of the POC test strips were validated by adding different concentrations of standards to the negative samples and calculating their recoveries through the addition of different concentrations of actual samples (5, 10, 60 μg/kg) to the negative samples. As summarized in Table 1, the mean recoveries ranged from 99.92 % to 102.3 %, with coefficients of variation below 10.2 %. These results demonstrate the high accuracy and reproducibility of the proposed POC LFIS platform for detecting ZEN in complex agricultural matrices.

3.7. Practical application of POC LFIA

5.0 g of negative cornmeal were ground and added to 20 mL of aqueous methanol (70 %). The mixture was stirred for 30 min on a

Table 2
Determination of ZEN in actual Cornflour seed samples using the MAF POC LFIA and confirmed by the LC-MS/MS method.

Sample NO.	POC LFIA (μg/Kg)	LC-MS/MS
1	-	-
2	-	-
3	-	-
4	-	-
5	-	-
6	-	-
7	-	-
8	6.27	6.50
9	-	-
10	-	-

magnetic stirrer to ensure adequate mixing. The supernatant was then centrifuged at 2800 ×g for 10 min, and various concentrations of ZEN standard solutionrations (0, 0.2, 1, 5, 25, and 100 μg/kg) were added to the sample. Fig. 5 showed that the T/C ratio decreases with increasing concentration of ZEN standard, and the results still exhibit a good linear relationship in the actual sample testing.

10 samples of cornflour from various regions of mainland China were tested using test strips. The results (Table 2) indicated that one sample tested positive (6.27 μg/kg), and these results were highly consistent with those obtained using the large-scale instrument LC-MS/MS, confirming the reliability and applicability of the proposed method for practical detection.

3.8. Comparison with reported ZEN detection methods

To further illustrate the advantages of our proposed method, we compared the analytical performance of the developed MAF-LFIA with several previously reported methods for ZEN detection (Table 3). Traditional instrumental methods such as HPLC and UHPLC-MS/MS generally achieve reliable quantification with LOQs in the range of 0.5–10 ng/mL, but they require laborious pretreatment and long analysis time, making them unsuitable for rapid on-site monitoring. Aptamer- or chemiluminescence-based sensors usually provide improved sensitivity (LOD of 2–3 ng/mL) and broad linear ranges; however, their operation involves multiple incubation or signal amplification steps, which limits their field applicability. Conventional LFIA platforms allow rapid visual readout within minutes, but their detection limits are often above 0.5 ng/mL, restricting their application in trace-level monitoring.

In contrast, our MAF-LFIA exhibits an ultralow detection limit of 0.0021 ng/mL, which is one to two orders of magnitude lower than most reported LFIA and biosensor-based methods. Meanwhile, the assay time is only 5 min, far shorter than that of chromatographic techniques and comparable to rapid immunoassays. Importantly, the MAF material not only overcomes the ACQ drawback of conventional fluorescent probes but also enables simple self-assembly with antibodies, thereby avoiding the use of chemical crosslinkers. This unique mosaic assembly preserves antibody activity and ensures targeted Fab exposure, enabling both high recovery (99.92–102.3 %) and excellent reproducibility (CV < 10.2 %). These results demonstrate that the MAF-LFIA not only overcomes the limitations of conventional LFIA but also provides a more sensitive and robust alternative to existing instrumental and biosensor approaches for rapid ZEN detection in agricultural products.

4. Conclusion

In this study, we developed a Zr^{4+}-based AIE metal-organic framework (MAF) that amplifies AIEgen fluorescence while enabling oriented, crosslinker-free assembly of anti-ZEN monoclonal antibodies. Simple mixing of MAF with the antibody yielded probes in which the Fc region is embedded within the framework and the Fab region remains exposed, thereby preserving antibody activity and enhancing target recognition. Integrated into a competitive lateral flow immunoassay, the MAF probe enabled rapid (5 min), highly sensitive and specific point-of-care detection of ZEN, with a limit of detection of 0.0021 ng/mL (corresponding to approximately 0.42 ng/g in corn samples), recoveries of 99.9–102.3 %, and coefficients of variation below 10.2 % in spiked cornmeal. Results for cornmeal samples were in good agreement with LC-MS/MS analysis, demonstrating the robustness of the assay. Overall, this MAF-based strategy offers a compact and generalizable platform that can be extended to immunoassays for other mycotoxins in complex food matrices.

CRediT authorship contribution statement

Qingqing Yang: Investigation, Funding acquisition, Formal analysis, Data curation. **Daohong Zhang:** Writing – review & editing, Methodology. **Chengchen Pang:** Writing – review & editing, Writing – original draft, Methodology, Investigation, Formal analysis, Data curation, Conceptualization. **Chunlei Yu:** Supervision. **Kunying Nie:** Writing – review & editing, Methodology. **Haitao Xu:** Supervision, Software, Methodology. **Keyun Ren:** Supervision, Software, Investigation.

Funding

The authors offer their gratitude to the National Natural Science Foundation of China and Scientific and Technological Research Council of Turkey for providing financial support within Project 32161133008, Project 121N859 and Department of Science and Technology of Shandong Provincial (Project 2022TSGC0055).

Table 3
Comparison of analytical performance of the proposed MAF-LFIA with previously reported methods for zearalenone (ZEN) detection.

Method	Sample	LOD / LOQ	Detection Range	Assay Time	Other performance	Reference
DNA-hydrogel + bimetallic MOFzyme aptasensor (colorimetric)	Corn & soybean	LOD：0.8 pg/mL	0.001–200 ng/mL	30–40 min	Recoveries：94.0–109.0 %	Sun et al. (2022)
Photothermal LFIA (BP-Au nanocomposite)	Cereals	LOD：4.3 pg/mL	10 pg/mL – 10^6 pg/mL	Minutes	Recoveries：91.8–120.2 %	Zhang et al. (2023)
Quantum dot-based fluorescent quenching LFA	Corn	LOD：0.58 ng/mL	0.78–25 ng/mL	Minutes	Recoveries：83.1–93.6 %	Chen et al. (2019)
Mesoporous silica/AuNPs SERS aptasensor	Corn	LOD：0.0064 ng/mL	3–200 ng/mL	~1 h	High sensitivity; good linearity	Guo et al. (2023)
Fab-phage ELISA	Corn, wheat, feed	LOD：0.03 ng/mL	0.07–3.89 ng/mL	2–3 h	High specificity	Chen et al. (2025)
Immunomagnetic beads chemiluminescence immunoassay	Grains & feed	LOD: 0.01 ng/mL	0.03–2.43 ng/mL	~1 h	Recoveries: 85.15–102.60 %;	Zhang et al. (2021)
MAF-LFIA (this work)	Cornmeal	LOD: 0.0021 ng/mL	0.315–5 ng/mL	~5 min	Recoveries: 99.9–102.3 %	This study

Declaration of Competing Interest

The authors declare that they have no known competing financial interests or personal relationships that could have appeared to influence the work reported in this paper.

Data Availability

Data will be made available on request.

References

Alt, K., Carraro, F., Jap, E., Linares-Moreau, M., Riccò, R., Righetto, M., Bogar, M., Amenitsch, H., Hashad, R.A., Doonan, C., Hagemeyer, C.E., Falcaro, P., Falcaro, P., 2022. Self-assembly of oriented antibody-decorated metal–organic framework nanocrystals for active-targeting applications. Adv. Mater. 34 (21), 2106607.

Bian, L., Li, Z., He, A., Wu, B., Yang, H., Wu, Y., Hu, F., Lin, G., Zhang, D., 2022. Ultrabright nanoparticle-labeled lateral flow immunoassay for detection of anti-SARS-CoV-2 neutralizing antibodies in human serum. Biomaterials 288, 121694.

Caihong, W., Jie, G., Hongliang, T., 2018. Integrated antibody with catalytic metal-organic framework for colorimetric immunoassay. ACS Appl. Mater. Interfaces 10 (30), 25113–25120.

Chen, Y., Fu, Q., Xie, J., Wang, H., Tang, Y., 2019. Development of a high sensitivity quantum dot-based fluorescent quenching lateral flow assay for the detection of zearalenone. ANAL BIOANAL CHEM 411 (10), 2169–2175.

Chen, Y., Liu, X., Li, J., Liu, X., 2025. Development of a sensitive enzyme immunoassay using phage-displayed antigen-binding fragments for zearalenone detection in cereal samples. Foods 14, 746.

Chua, M.H., Hui, B.Y.K., Chin, K.L.O., Zhu, Q., Liu, X., Xu, J., 2023. Recent advances in aggregation-induced emission (AIE)-based chemosensors for the detection of organic small molecules. Mater. Chem. Front 7 (22), 5561–5660.

Feng, Y., Wang, H., Zhang, S., Zhao, Y., Gao, J., Zheng, Y., Zhao, P., Zhang, Z., Zaworotko, M.J., Cheng, P., Ma, S., Chen, Y., 2019. Antibodies@MOFs: an in vitro protective coating for preparation and storage of biopharmaceuticals. Adv. Mater. 31 (2), 1805148.

Gopal, A., Yan, L., Kashif, S., Munshi, T., Roy, V.A.L., Voelcker, N.H., Chen, M., 2021. Biosensors and point-of-care devices for bacterial detection: rapid diagnostics informing antibiotic therapy. Adv. Healthc. Mater. 10, 2101546.

Guo, Z., Gao, L., Yin, L., Arslan, M., El-Seedi, H.R., Zou, X., 2023. Novel mesoporous silica surface loaded gold nanocomposites SERS aptasensor for sensitive detection of zearalenone. Food Chem. 403, 134384.

Hou, Q., Zhou, S., Wei, Y., Caro, J., Wang, H., 2020. Balancing the grain boundary structure and the framework flexibility through bimetallic metal–organic framework (MOF) membranes for gas separation. J. Am. Chem. Soc. 142 (21), 9582–9586.

Mei, J., Leung, N.L., Kwok, R.T., Lam, J.W., Tang, B.Z., 2015. Aggregation-induced emission: Together We Shine, United We Soar! Chem. Rev. 115 (21), 11718–11940.

Obremski, K., Trybowski, W., Wojtacha, P., Gajęcka, M., Tyburski, J., Zielonka, Ł., 2016. The effect of zearalenone on the cytokine environment, oxidoreductive balance and metabolism in Porcine Ileal Peyer's Patches. Toxins 12 (6), 350.

Pang, Y., Yang, Z., Liu, X., Shen, X., Xu, Z., Lei, H., Zhao, H., Li, X., 2023. A robust and sensitive enhanced immunochromatographic assay based on UiO-66-NH2 @Au for simultaneous detection of carbofuran and 3-hydroxy-carbofuran in fruits and vegetables. Sens. Actuators B Chem. 397, 134633.

Pang, C., Yuan, B., Ren, K., Xu, H., Nie, K., Yu, C., Liu, Z., Zhang, Y., Ozkan, S.A., Yang, Q., 2024. Activates B lymphocytes and enhanced immune response: a promising adjuvant based on PLGA nanoparticle to improve the sensitivity of ZEN monoclonal antibody. Talanta 274, 126005.

Pršir, K., Matić, M., Grbić, M., Mohr, G.J., Krištafor, S., Steinberg, I.M., 2023. Naphthalimide-piperazine derivatives as multifunctional "On" and "Off" fluorescent switches for pH, Hg^{2+} and Cu^{2+} ions. Molecules 28 (3), 1275.

Shen, X.-A., Zhou, H., Chen, X., Wu, J., Su, Y., Huang, X., Xiong, Y., 2024. Janus plasmonic-aggregation induced emission nanobeads as high-performance colorimetric–fluorescent probe of immunochromatographic assay for the ultrasensitive detection of staphylococcal enterotoxin B in milk. BIosens. Bioelectron 261, 116458.

Singh, S., Bhatt, D., Deep, A., Tiwari, U.K., 2024. An antibody conjugated NH2-MIL-101 (Fe) metal-organic framework based optical biosensor for sensitive detection of lead ions. Microchem. J. 199, 110122.

Snigdhamayee, R., Rani, N.S., Sivakumar, S.V., 2024. Efficiency boost in non-doped blue organic light-emitting diodes: harnessing aggregation-induced emission-a comprehensive review. J. Mater. Chem. C 12 (3), 765–818.

Sun, Y., Qi, S., Dong, X., Qin, M., Zhang, Y., Wang, Z., 2022. Colorimetric aptasensor targeting zearalenone developed based on the hyaluronic Acid-DNA hydrogel and bimetallic MOFzyme. Biosens Bioelectron 212, 114366.

Wang, J., Li, M., Zhang, W., Gu, A., Dong, J., Li, J., Shan, A., 2018b. Protective effect of N-acetylcysteine against oxidative stress induced by zearalenone via mitochondrial apoptosis pathway in SIEC02 cells. Toxins 10 (10), 407.

Wang, C., Sudlow, G., Wang, Z., Cao, S., Jiang, Q., Neiner, A., Morrissey, J.J., Kharasch, E.D., Achilefu, S., Singamaneni, S., 2018a. Metal-organic framework encapsulation preserves the bioactivity of protein therapeutics. Adv. Healthc. Mater. 7 (22), 1800950.

Wang, X., Yang, C., Jiang, W., Zhang, M., Li, R., Lin, Y., Wang, Q., 2023. Rapid quantitative detection of okadaic acid in shellfish using lanthanide-labelled fluorescent-nanoparticle immunochromatographic test strips. Food Control 148, 109635.

Wu, W., Li, Y., Song, P., Xu, Q., Lei, D., Wang, J., Fu, B., Kong, W., 2024. UiOL@AIEgens-assisted lateral flow immunosensor for the ultrasensitive dual-modal point-of-care detection of aflatoxin B1. J. Hazard. Mater. 465, 133103.

Yin, X., Dou, L., Yao, X., Liu, S., Zhang, L., Zhao, M., Su, L., Sun, J., Wang, J., Zhang, D., 2022. Controllable assembly metal-organic frameworks and gold nanoparticles composites for sensitive immunochromatographic assay. Food Chem. 367, 130737.

Zhang, L., Chen, X., Bhattacharjee, P., Shi, Y., Guo, L., Wang, S., 2020a. Molecular characterization of a novel strain of Fusarium graminearum Virus 1 infecting Fusarium graminearum. Viruses 12 (3), 357.

Zhang, Y., Chen, G., Chen, X., Wei, X., Shen, X.A., Jiang, H., Li, X., Xiong, Y., Huang, X., 2024. Aggregation-induced emission nanoparticles facilitating multicolor lateral flow immunoassay for rapid and simultaneous detection of aflatoxin B1 and zearalenone. Food Chem. 447, 138997.

Zhang, B., Li, H., Li, Y., et al., 2021. A sensitive chemiluminescence immunoassay based on immunomagnetic beads for quantitative detection of zearalenone. Eur. Food Res. Technol. 247, 2171–2181.

Zhang, S., Razmjou, A., Azadi, S., Bazaz, S.R., Shrestha, J., Jahromi, M.A.F., Warkiani, M. E., 2020c. Metal–organic framework-enhanced ELISA platform for ultrasensitive detection of PD-L1. ACS Appl. Bio Mater. 3 (7), 4148–4158.

Zhang, J., Li, Y., Chai, F., Li, Q., Wang, D., Liu, L., Tang, B.Z., Jiang, X., 2022a. Ultrasensitive point-of-care biochemical sensor based on metal-AIEgen frameworks. Sci. Adv. 8 (30), eabo1874.

Zhang, Y., Wang, Z., Qu, X., Zhou, Jie, Yang, H., Wang, W., Yang, C., 2023b. A photothermal lateral flow immunoassay for zearalenone with high sensitivity and wide detection range. Sens. Actuators B Chem 390, 0925–4005, 133909.

Zhang, H., Zhao, Z., Turley, A.T., Wang, L., McGonigal, P.R., Tu, Y., Li, Y., Wang, Z., Kwok, R.T.K., Lam, J.W.Y., Tang, B.Z., 2020b. Aggregate science: from structures to properties. Adv. Mater. 32 (36), 2001457.

Zhu, Z., Wen, J., Xu, Y., Pei, H., Li, D., Tang, M., Bai, P., He, J., Yang, Z., Chen, L., 2022. Therapeutic efficacy of an injectable formulation of purinostat mesylate in SU-DHL-6 tumour model. Ann. Med. 54 (1), 743–753.

Zhu, L., Wu, Q., Mei, X., Li, Y., Yang, J., 2023. Paper-based microfluidic sensor array for tetracycline antibiotics discrimination using lanthanide metal–carbon quantum dots composite ink. Adv. Compos. Hybrid. Mater. 6 (6), 221.

Zhu, Q.L., Xu, Q., 2014. Metal–organic framework composites. Chem. Soc. Rev. 43 (16), 5468–5512.

Zielonka, Ł., Gajęcka, M., Lisieska-Żołnierczyk, S., Dąbrowski, M., Gajęcki, M.T., 2020. The Effect of different doses of zearalenone in feed on the bioavailability of zearalenone and alpha-zearalenol, and the concentrations of estradiol and testosterone in the peripheral blood of pre-pubertal gilts. Toxins 12 (3), 144.